

Article

An Experimental Investigation of WAG Injection in a Carbonate Reservoir and Prediction of the Recovery Factor Using Genetic Programming

Mirosław Wojnicki ^{1,*}, Jan Lubaś ¹, Mateusz Gawroński ², Sławomir Szufflita ¹, Jerzy Kuśnierczyk ¹
and Marcin Warnecki ¹

¹ Oil and Gas Institute—National Research Institute, 31-503 Krakow, Poland; lubas@inig.pl (J.L.); szufflita@inig.pl (S.S.); kusnierczyk@inig.pl (J.K.); warnecki@inig.pl (M.W.)

² Department of Robotics and Mechatronics, AGH University of Science and Technology, 30-059 Krakow, Poland; matgawr@agh.edu.pl

* Correspondence: wojnicki@inig.pl

Abstract: Production from mature oil fields is gradually declining, and new discoveries are not sufficient to meet the growing demand for oil products. Hence, enhanced oil recovery is emerging as an essential link in the global oil industry. This paper aims to recognize the possibility of increasing oil recovery from Polish carbonate reservoirs by the water alternating gas injection process (WAG) using various types of gases, including CO₂, acid gas (a mixture of CO₂ and H₂S of 70/30% vol/vol) and high-nitrogen natural gases occurring in the Polish Lowlands. A series of 17 core flooding experiments were performed under the temperature of 126 °C, and at pressures of 270 and 170 bar on composite carbonate cores consisting of four dolomite core plugs. Original reservoir rock and fluids were used. A set of slim tube tests was conducted to determine the miscibility conditions of the injected fluids with reservoir oil. The WAG process was compared to continuous gas injection (CGI) and continuous water injection (CWI) and was proven to be more effective. CO₂ WAG injection resulted in a recovery factor (RF) of up to 82%, where the high nitrogen natural gas WAG injection was less effective with the highest recovery of 70%. Based on the core flooding results and through implementing a genetic programming algorithm, a mathematical model was developed to estimate recovery factors using variables specific to a given WAG scheme.

Keywords: enhanced oil recovery; WAG; carbonate reservoir; CO₂; acid gas; high-nitrogen natural gas; water alternating gas; EOR; recovery factor; genetic programming



Citation: Wojnicki, M.; Lubaś, J.; Gawroński, M.; Szufflita, S.; Kuśnierczyk, J.; Warnecki, M. An Experimental Investigation of WAG Injection in a Carbonate Reservoir and Prediction of the Recovery Factor Using Genetic Programming. *Energies* **2022**, *15*, 2127. <https://doi.org/10.3390/en15062127>

Academic Editor: Reza Rezaee

Received: 20 January 2022

Accepted: 13 March 2022

Published: 14 March 2022

Publisher's Note: MDPI stays neutral with regard to jurisdictional claims in published maps and institutional affiliations.



Copyright: © 2022 by the authors. Licensee MDPI, Basel, Switzerland. This article is an open access article distributed under the terms and conditions of the Creative Commons Attribution (CC BY) license (<https://creativecommons.org/licenses/by/4.0/>).

1. Introduction

The oil recovery factor in conventional reservoirs varies from field to field since it depends on many different variables. The worldwide average is about 30% IOIP (initial oil in place) which means that there is great potential to recover more [1]. That is why enhanced oil recovery (EOR) has been one of the most investigated areas in the petroleum industry in the last decades. Tremendous work has been done so far which has resulted in a vast range of published papers concerning lab-scale research, reservoir modelling, and the outcome of field applications of different EOR methods [2,3]. Despite that, the ultimate profit from EOR applications is below expectation (<10% of total production), and recent studies show that EOR is still in the top priority research and innovation areas in the energy industry [4]. The need to further explore EOR concepts comes from the fact that every EOR process is strongly case-specific and it is difficult to make an analogy to another case, thus requiring specific research, optimization, expertise, and trial field demonstration.

Carbonate reservoirs are of special interest, because they contain more than 60% of the world's remaining conventional oil reserves and account for over 30% of the world's daily oil production [5–8]. Due to the complex oil recovery process in carbonates caused by their

unfavorable reservoir characteristics, recovery factors are even lower with an average of 20% [9–11]. The above include high heterogeneity, mixed- to oil-wet conditions, and dual permeability—poor in rock matrices and high in fractures [12,13].

Most of the EOR projects in carbonates are gas injections (nearly 60%), and the vast majority use CO₂ (continuously or alternately with water). Currently, a majority of CO₂-EOR projects utilize CO₂ from natural sources, but as global discussion on climate change and worldwide efforts on carbon emission reduction intensifies, it is expected that anthropogenic CO₂ sources will be more frequently used. Hydrocarbon gas injection projects have a significantly lower contribution for EOR in carbonates. Others such as nitrogen or acid gas (mixture of H₂S and CO₂) are even less common [1,3,14].

However, EOR gas injection poses significant challenges connected with the high mobility ratio (caused by the significantly lower dynamic viscosity of the injected gas compared to reservoir oil), including viscous fingering and early breakthrough of the injected fluid into production wells [15,16].

To counteract that, a Water Alternating Gas (WAG) injection method was initially designed to control gas mobility and stabilize the gas displacement front during continuous gas injection (CGI) and finally improve sweep efficiency. The method, which combines CGI and waterflooding (continuous water injection—CWI) methods, was first implemented in 1956 in the North Pembina field (Alberta, Canada), and since then has been effectively used worldwide [16–19]. The combination of improved microscopic displacement of CGI with an improved macroscopic sweep of CWI led, in most cases, to enhanced oil recovery. Water slugs stabilize the displacement front and help to sweep crude oil from the lower part of the reservoir [20]. A further essential benefit of WAG is that less gas is required for injection, in favor of the usually cheaper water. In the WAG method, both water and gas are injected to the same well. There are different WAG injection schemes where, e.g., water and gas are injected simultaneously (SWAG) [21,22], a huge slug of gas is followed by a number of conventional WAG cycles—HWAG [23], or the volume of injected gas is gradually reduced over time—TWAG [24].

Gas can be injected under miscible (MWAG) or immiscible (IWAG) conditions that are differentiated by the Minimum Miscibility Pressure (MMP). When the injection pressure is slightly lower than MMP, it is hard to distinguish between miscible and immiscible types because of the subsequent mass transfer mechanisms involved (swelling/stripping), and such conditions should be referred to as “near-miscible” regime (nMWAG) [21,25]. Both MWAG and nMWAG are considered more effective than IWAG [17,26], but many studies revealed that IWAG is also efficient in enhancing oil recovery [27,28]. Miscibility development is not always required for successful WAG implementation, but helps to achieve better results in most cases [10]. The general scheme of WAG injection is shown in Figure 1.

WAG injection has been comprehensively studied with a particular consideration of factors affecting its performance such as reservoir parameters including wettability [29,30] heterogeneity [31–33], and fractures [34], injected fluid parameters including water salinity [35–37] and gas type [15,38], the WAG parameters including the WAG ratio [39,40], the number of cycles, slug sizes [41,42], the timing of injection [43], and finally the injection rates of the gas and water phases [11].

The cyclic nature of WAG leads to an increase in water saturation during the water injection half cycle and a decrease of water saturation during the gas injection half cycle involving associated hysteresis phenomena resulting in complex three phase-flow which makes the prediction of WAG performance very difficult. This was extensively studied by Fatemi, Sohrabi, and Shahverdi [44,45].

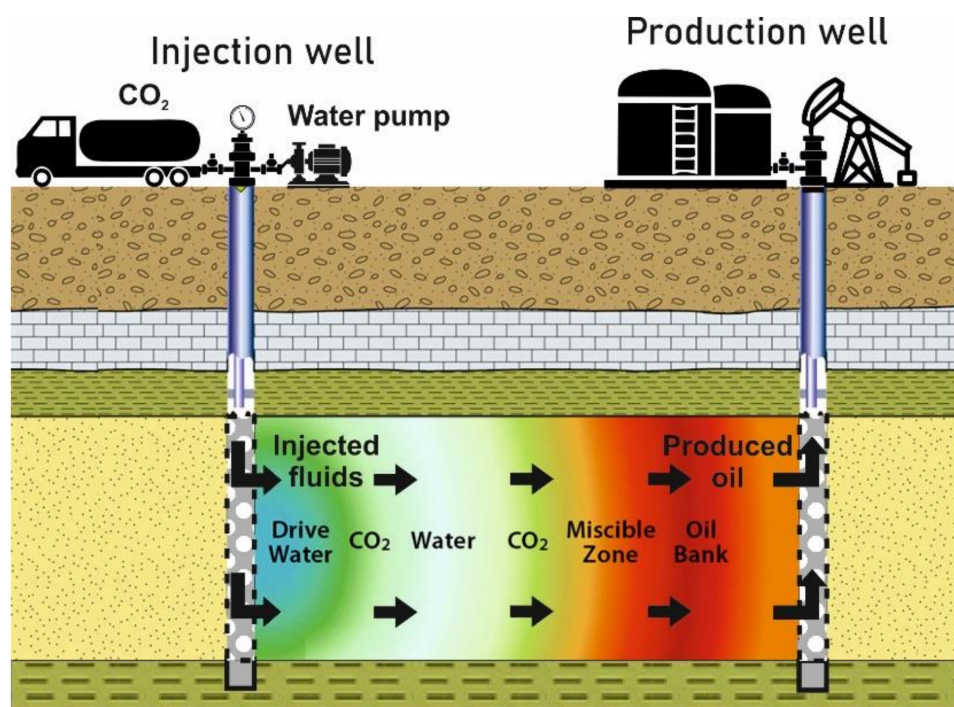


Figure 1. General scheme of WAG injection (miscible).

Physical simulation of the WAG process in the laboratory is generally done using the core flooding test, which is also used in the presented paper. Several important works were also conducted using micromodel visualization [46–49]. Over the years, a number of experimental studies has been performed in mixed wet carbonates, revealing different process issues and enabling the more effective use of WAG in complex reservoir conditions.

However, considering that WAG process efficiency is strongly site-specific, there is a gap concerning its suitability in the specific conditions of mixed-wet and fractured carbonate sour crude oil reservoirs of the Polish Lowlands. The novelty of the research is defined by the type of crude oil, reservoir conditions, and injected gases used. There is a lack of published WAG experimental data for such kind of settings. The previous study of the authors focused on evaluating high-nitrogen sour natural gas WAG injection and the impact of fractures on its efficiency [50]. Whereas the current work aims to evaluate the efficiency of four different types of gases in WAG injection and focus on empirical modelling of the oil recovery factor based on experimental data using evolutionary algorithms. Genetic programming was used to generate a correlation to predict the oil recovery factor as a function of variables defining core flooding experiments, i.e., injected gas composition, pressure, and the gas to water ratio in the injected fluid stream.

The estimated oil recovery factor is one of the most significant parameters for an operator when selecting the proper EOR method. The recovery factor is affected by several engineering and geological aspects, that make the estimation of the RF complex. RF estimation based on experimental data could be applied strictly in the tested conditions (or very similar) characterized by reservoir fluids, rock type, temperature, or flow conditions in porous media (e.g., natural fractures).

Implementation of evolutionary algorithms in the petroleum industry is widespread and concentrates on parameter estimation, correlation generation, and predictive analytics. They are particularly useful in solving problems where the relationships between variables are unknown or poorly understood [51,52]. Examples of the application of evolutionary algorithms in reservoir engineering include modelling and production optimization [53–55], estimation of effectiveness and optimization of EOR methods (including WAG) [56–59], estimating values of parameters such as MMP [60], the formation volume factor [61] or the emulsion viscosity [62], and issues related to the reservoir development [63–67].

2. Materials and Methods

Core flooding experiments were performed using original reservoir rock saturated with original reservoir fluids (brine, live oil) at thermobaric conditions of one of the major Polish oil reservoirs located in the Polish Lowlands. The reservoir has been developed in naturally fractured Late Permian Zechstein carbonates (mainly dolomites) of the Main Dolomite formation. The carbonates are both the source and the reservoir of the rocks and are sealed above and below by evaporites (Werra–Strassfurt cyclothemes) creating a closed petroleum system. This results in the presence of residual organic matter in reservoir rock, strongly affect the rocks' wettability leading to mixed-wet conditions. Experimental studies of WAG injection efficiency using very high-nitrogen natural gas (KG) for the same conditions were performed in a previous study [50]. In the referenced work, issues concerning reservoir characteristic rock material core flooding and the experimental process are described in detail. In the current study 3 new gas types, that are likely to be used in the WAG process, were tested. These include carbon dioxide, acid gas—a mixture of CO_2 and H_2S of 70/30% vol/vol corresponding to post-process gas from an amine sweetening plant (AG)—and nitrogen natural gas (MG).

2.1. Reservoir and Injected Fluids

Reservoir fluid was prepared individually prior to each core flooding and slim tube experiment by physical recombination from separator oil and gas samples. To ensure accurate recombination of reservoir fluid and determine the parameters required to correctly design, perform, and balance the experiments a full spectrum of PVT analyses was performed. Initial and current PVT data were used to develop a reservoir fluid model. The phase diagram of the considered reservoir fluid is shown in Figure 2.

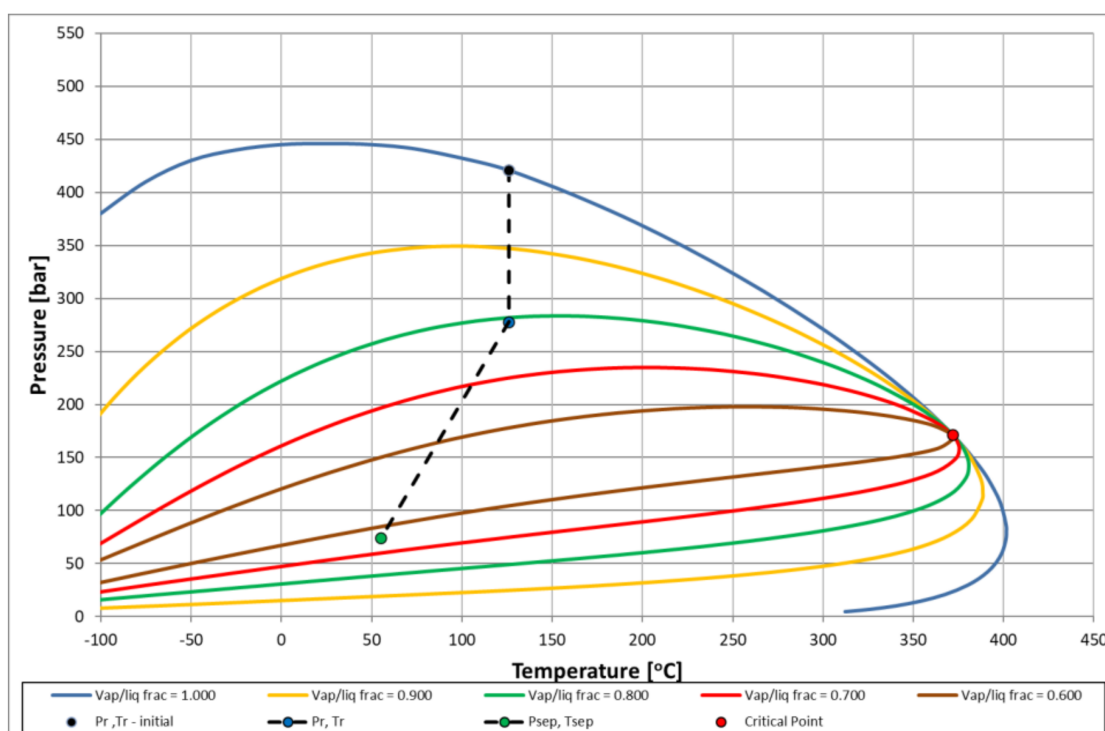


Figure 2. Phase diagram of reservoir fluid.

As can be seen from the PT diagram the initial reservoir pressure lies in the bubble point curve that indicates saturated oil conditions, along with an isothermal pressure depletion caused by the ongoing production reservoir fluid which reached the two-phase region. The dashed line indicates the path from the initial reservoir, through the current reservoir to the separator conditions.

The oil is light and sour crude oil with dynamic viscosity of 0.5 cP, and density of 0.65 g/cm³ at reservoir conditions (P = 270 bar, T = 126 °C). The simplified composition of reservoir fluid is presented in Table 1.

Table 1. Composition of reservoir (live) oil.

Component	N ₂	CO ₂	H ₂ S	C ₁	C ₂	C ₃	C ₄	C ₅	C ₆	C ₇	C ₈	C ₉	C ₁₀ –	C ₁₁	C ₁₂	C ₁₃	C ₁₄	C ₁₅₊
Mol %	30.4	0.5	4.8	19.3	3.4	2.6	2.3	3.2	2.4	2.8	3.1	2.9	2.7	2.0	1.7	1.6	1.4	13.1

The water phase used for core saturation, as well as the injection fluid in the WAG water cycle was sampled from the separator of the same well as the hydrocarbon fluids and proved to have pH of 7.9 and density of 1.006 g/cm³. Its dynamic viscosity at test conditions (P = 270 bar, T = 126 °C) was 0.411 cP. The simplified composition of formation water is tabulated in Table 2.

Two types of nitrogen rich natural gases were used. The first one abbreviated KG is characterized by a very high nitrogen (~87%) content and the presence of hydrogen sulfide (2.7%) and carbon dioxide (1.2%). Its dynamic viscosity at the test conditions (P = 270 bar, T = 126 °C) was 0.0273 cP. The simplified compositional analysis of injected gas is shown in Table 3. It was sampled from the separator during a production test in the undeveloped gas field.

The second one abbreviated MG has lower nitrogen and carbon dioxide content but much higher methane content. Its density is 1.164 kg/m³, and the dynamic viscosity at test conditions (P = 270 bar, T = 126 °C) is 0.0260 cP. It was sampled from the producing gas field located in the vicinity of the considered oil field. The simplified compositional analysis of injected gas is shown Table 4.

Table 2. Composition of formation water.

Total Salinity (g/L)	Cation (g/L)						Anion (g/L)				
	Na ⁺	K ⁺	Mg ²⁺	Ca ²⁺	NH ₄ ⁺	Cl [−]	Br [−]	SiO ₃ ^{2−}	HCO ₃ [−]	SO ₄ ^{2−}	S ^{2−}
8.932	2.03	0.462	0.062	0.389	0.259	5.265	0.037	0.013	0.177	0.147	0.505

Table 3. Simplified composition of KG natural gas.

Density (kg/m ³)	Component Concentration (%mol)								
	N ₂	H ₂ S	CO ₂	H ₂	C ₁	C ₂	C ₃	C ₄₊	
1.2507	86.9	2.7	1.2	1.1	5.6	0.8	0.7	1	

Table 4. Simplified composition of MG natural gas.

Density (kg/m ³)	Component Concentration (%mol)						
	N ₂	H ₂ S	CO ₂	C ₁	C ₂	C ₃	C ₄₊
1.164	58.6	3.3	0.3	28.7	4.7	2.6	0.7

2.2. Rock Material

In the core flooding experiments original reservoir rock from the Upper Permian Main Dolomite Formation of the Zechstein Basin in western Poland was used. Reservoir rock samples were taken from the pay zone cored interval of one of the producing wells at a depth of around 3000 m. Mineral composition was quite uniform and consisted mainly of dolomite (~83%) with ankerite (~16%), anhydrite (~1%), and quartz (~0.5%) [50]. From the whole drilling of core samples, core plugs with 2.54 in diameter, and length of ~5–6 cm, were drilled horizontally. Then they were end faced, polished, cleaned, and dried. Most of the core plug preparation procedures were conducted following the guideline from API RP40 [68]. After that, their parameters such as absolute permeability (using a steady-state

nitrogen permeameter), effective porosity (using a helium porosimeter) pore volume, bulk density, as well as grain density were determined. The samples with similar parameters were selected and grouped into composite cores consisting of four core plugs. Core plugs were arranged with Langaas criterion (decreasing permeability in the flow direction), such that the core with the highest permeability was placed at the inlet and the core with the lowest permeability at the outlet [69]. A set of parameters characterizing exemplary composite cores is presented in Table 5.

Six composite cores were assembled with the average porosity in the range of 23–30% and permeability of 70–80 mD. The basic parameters of the composite cores used in the core flooding tests are presented in Table 6. As the availability of the original reservoir rock samples from drilling cores is very limited, the composite cores were reused. Routine cleaning in a Soxhlet apparatus was replaced by dynamic mild cleaning using kerosene/heptane, DI water, and nitrogen to reduce the cleaning impact on the core properties. This involves injecting (in PT conditions) about 5 PV of kerosene, followed by about 5 PV of heptane, totaling 10 PV of solvent flooding. Then DI water was injected to remove dissolvable salts, followed by nitrogen which helps remove residues and dry out the sample. Directly after, cores were dried in the oven until they achieved a constant weight. Such an approach helps maintain and restore the original reservoir wettability in the carbonates [70].

Table 5. Individual core parameters of composite core no 1.

Core ID	Permeability	Effective Porosity	Core Volume	Grain Density	Length	Diameter
	[mD]	[%]	[cm ³]	[g/cm ³]	[cm]	[cm]
46	96.4	19.01	26.916	2.823	5.35	2.54
85	83.1	31.64	24.925	2.818	4.98	2.54
49	59.1	28.25	26.511	2.817	5.29	2.54
25	43.5	29.54	28.006	2.817	5.59	2.54
Composite core parameters						
Average permeability [mD]				70.5		
Average permeability [%]				27.1		
Composite core volume [cm ³]				106.4		
Composite core pore volume [cm ³]				28.8		
Composite core length				21.21		

Table 6. Properties of composite cores.

Composite Core No.	Length [cm]	Average Porosity [%]	Average Permeability [mD]	Pore Volume [cm ³]
1	21.21	27.1	70.5	28.8
2	21.73	30.4	77.3	33.0
3	21.95	24.6	72.1	26.4
4	22.30	22.7	80.7	25.7
5	21.40	24.6	80.4	26.7
6	22.15	28.7	77.0	31.8

2.3. Minimum Miscibility Pressure

Oil displacement through WAG gas injection is most effective when the injected gas is completely or near miscible with the oil in the reservoir. The main factor responsible for the increased oil displacement during miscible gas injection is the mass transfer of components between the flowing gas phase and the oil phase present in the reservoir. The efficiency of this process increases along with the miscibility of both phases. Immiscible WAG recovery mechanisms (also present in miscible injection) include oil volume expansion (oil swelling), oil viscosity reduction, 3-phase relative permeability, and oil film flow [71].

Fluids are considered miscible when they mix in all proportions to form a single homogeneous phase, so the miscibility is a physical condition between two (or more) fluids that permits them to mix in all proportions without the existence of any interface [72,73]. Under reservoir conditions of constant temperature and quasi-constant composition, a factor determining miscibility is pressure, and the lowest pressure at which the first or multiple-contact miscibility can be achieved is called the minimum miscibility pressure (MMP). It needs to be determined for each specific pair of fluids (reservoir oil and injected gas).

The slim tube method, which is the primary and most commonly used method for laboratory determination of MMP in industry, was used to determine MMP for the injected gas and reservoir oil. The slim tube is a one-dimensional model of the reservoir in the form of narrow and long stainless-steel tube packed with a porous material (typically with sand). This simple design allows multiple contact conditions between flowing fluids in a porous medium and provides dimensional dispersion free displacement of oil. Gravity override caused by the gravity effect is negligible because the tube is coiled, so that flow is basically horizontal. Tests are conducted at a constant reservoir temperature controlled by a thermostatic bath, where the tube is placed. The observation of the ongoing phenomena is possible through a mounted sight glass. Schematic diagram of the slim tube apparatus is shown in Figure 3.

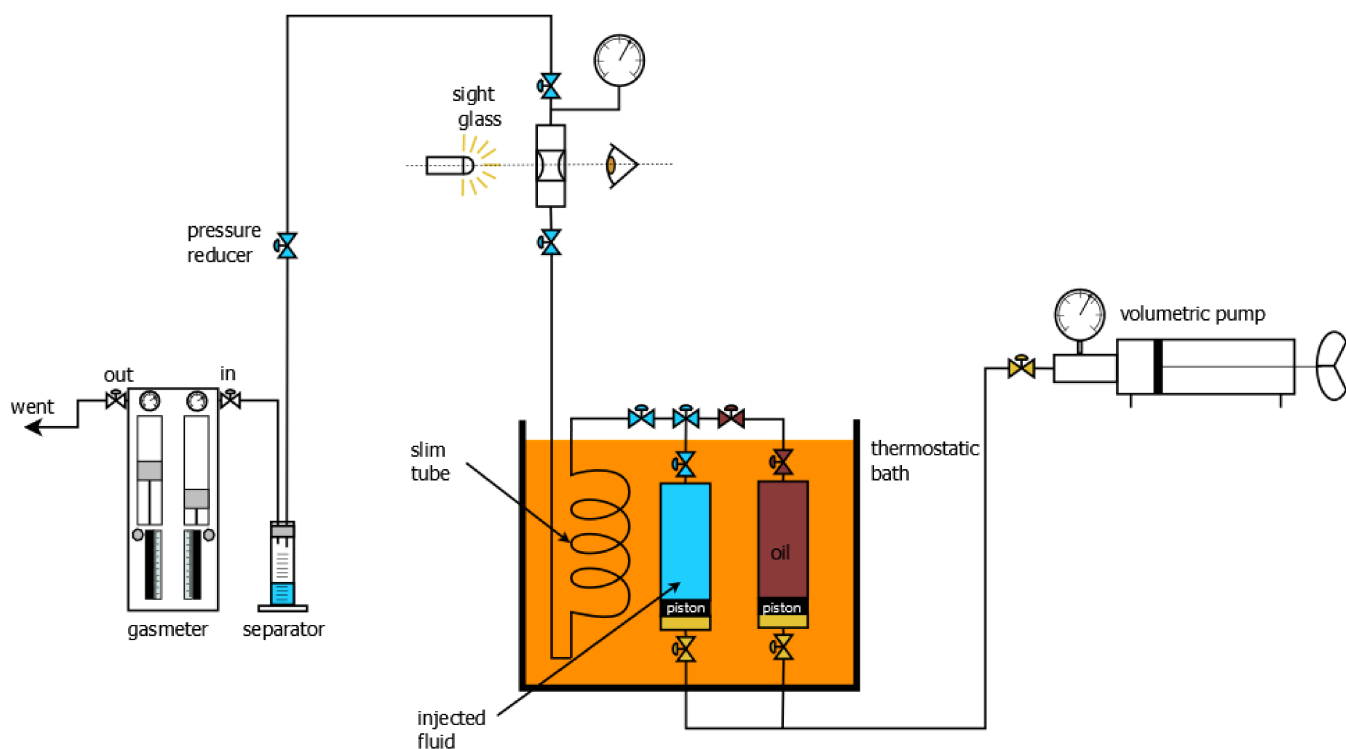


Figure 3. Schematic diagram of the slim tube set-up.

The test starts by saturating the porous media with reservoir oil. Then the oil is displaced by injecting gas at a constant rate and inlet pressure. The differential pressure between the inlet and outlet of the tube is so small compared to the pressure in the system that the displacement pressure is considered constant. The injected and produced fluid volumes are precisely monitored and measured during the test, which ends after injecting 1.2 pore volume (PV) of gas. Miscibility conditions are determined by conducting the displacement at various pressures and plotting the oil recoveries as a function of displacement pressure. The study is normally performed at between 4 to 6 test pressure. After every test the slim tube apparatus must be carefully cleaned with solvents and dried prior to subsequent saturation. Based on the plot observation, MMP could be identified as the pressure break

in the curve (the recovery-pressure curve starts to flatten when the displacement becomes near miscible). Some researchers use specific recovery factor, e.g., 90% at 1.2 PV of injected gas as MMP [74]. The specification of the slim tube apparatus setup used in the study is presented in Table 7.

Experimental MMP studies were performed for CO₂, AG, and MG. The tests for KG were not undertaken because miscibility conditions would be unlikely to occur, in the considered pressure range, due to the very high nitrogen content in KG. The basic parameters of the performed slim tube tests are presented in Table 8. The MMP was also double-checked via simulations in PVTsim software using the original reservoir fluid model.

Table 7. Slim tube setup properties.

Parameter	Setting
Length	25 m
Internal diameter	5 mm
Pore volume	174.659 cm ³
Porosity	15 D
Permeability	35%
Grain type	Quartz sand
Grain size	0.15–0.20 mm
Injection rate	
Temperature	126 °C

Table 8. Basic properties of Slim tube tests.

Test No.	Injected Gas	Oil Saturation Pressure [bar]	Gas Injection Pressure [bar]
1	CO ₂	130	140
2	CO ₂	160	170
3	CO ₂	200	210
4	CO ₂	280	290
5	CO ₂	330	340
6	CO ₂	420	430
7	AG	130	140
8	AG	160	170
9	AG	200	210
10	AG	280	290
11	AG	330	340
12	AG	420	430
13	MG	240	250
14	MG	280	290
15	MG	330	340
16	MG	420	430
17	MG	460	470

2.4. Coreflooding Process

In the core flooding experiments a customized and properly adapted PVT apparatus upgraded with an additional core-holder cell was used. The core holder was designed based on the analysis of the available technical solutions with a special focus on the specification of the experiments and conditions where it would be used. A radial core holder can accommodate cores with a diameter of 2.54 cm (1 inch) and length up to 25 cm. Composite cores were placed in a rubber sleeve and then in the core holder (Figure 4). Tightness protection between the sleeve and composite core was maintained by a pressurized water system.

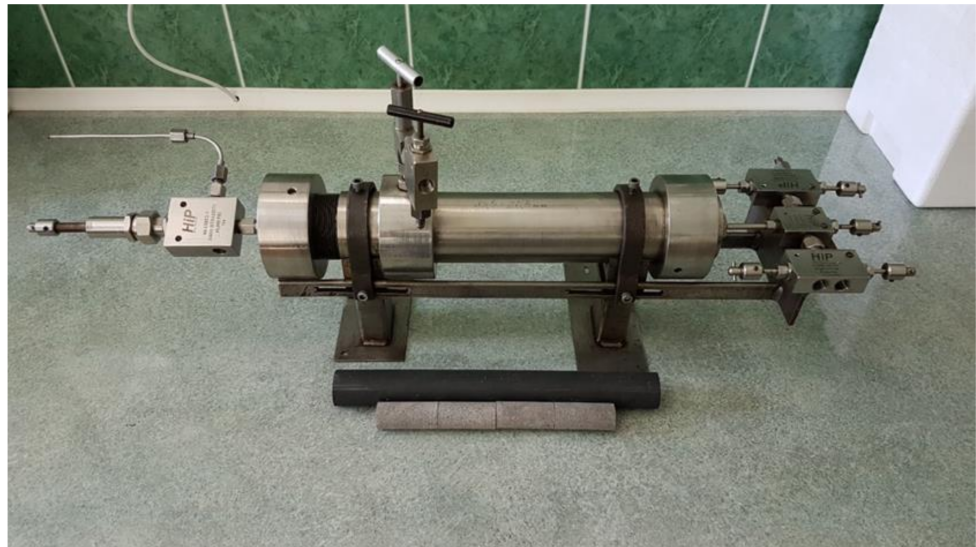


Figure 4. The core holder with rubber sleeve and core plugs forming the composite core.

A confining pressure of 100 bar higher than the test pressure was held during the injection. Stable temperature conditions ($126\text{ }^{\circ}\text{C} \pm 0.5\text{ }^{\circ}\text{C}$) for the horizontally placed core holder and fluid bearing pressure cells were maintained using a thermostatic air bath. The core holder has one inlet and one outlet port connected to the pressure and temperature transducers. The fluid flow was controlled through the set of precise HTHP valves. Produced liquids were measured using a graduated cylinder, while the produced gas was measured using a gas meter. The proper configuration of an experimental set-up and its features such as dead volumes, location of PT transducers, location and type of pressure connections are essential for the accuracy of the volume measurements of injected and withdrawn fluids, and thus for the reliability and consistency of the obtained results. Therefore, special attention was paid to the correct design and then the verification and testing of the solutions used. Figure 5 shows a simplified scheme of the core flooding experimental setup.

Initially, the composite core was saturated with reservoir water to reach the preset pressure, and the pore volume (PV) was determined. Then, the composite core was flooded with live oil under the given test pressure, with constant flow rate $q = 0.3\text{ cm}^3/\text{min}$ to determine the irreducible water saturation, and subsequently the hydrocarbon saturation—hydrocarbon pore volume (PV_{HC}). The total amount of injected fluids during coreflooding experiments was $1.2\text{ PV}_{\text{HC}}$. The injection flow rate was fixed at $0.07\text{ cm}^3/\text{min}$, which in the composite core resulted in velocity within the range $2.5 \div 3.3\text{ cm/h}$. In the WAG process, the injection cycle started with gas in most of the experiments, and the slug size was $0.2\text{ PV}_{\text{HC}}$. A total of 17 coreflooding experiments was conducted, including 5 variants differing in injection scheme/WAG ratio (CGI; WAG 1:1, 1:2, 2:1) and injection pressure (270 and 170 bar) for each newly tested gas (MG, AG and CO_2), and two supplementary tests to complement previously conducted studies for KG gas [50]. To compare WAG process efficiency, tests with continuous gas injection were performed. The properties of the core flooding experiments are summarized in Table 9.

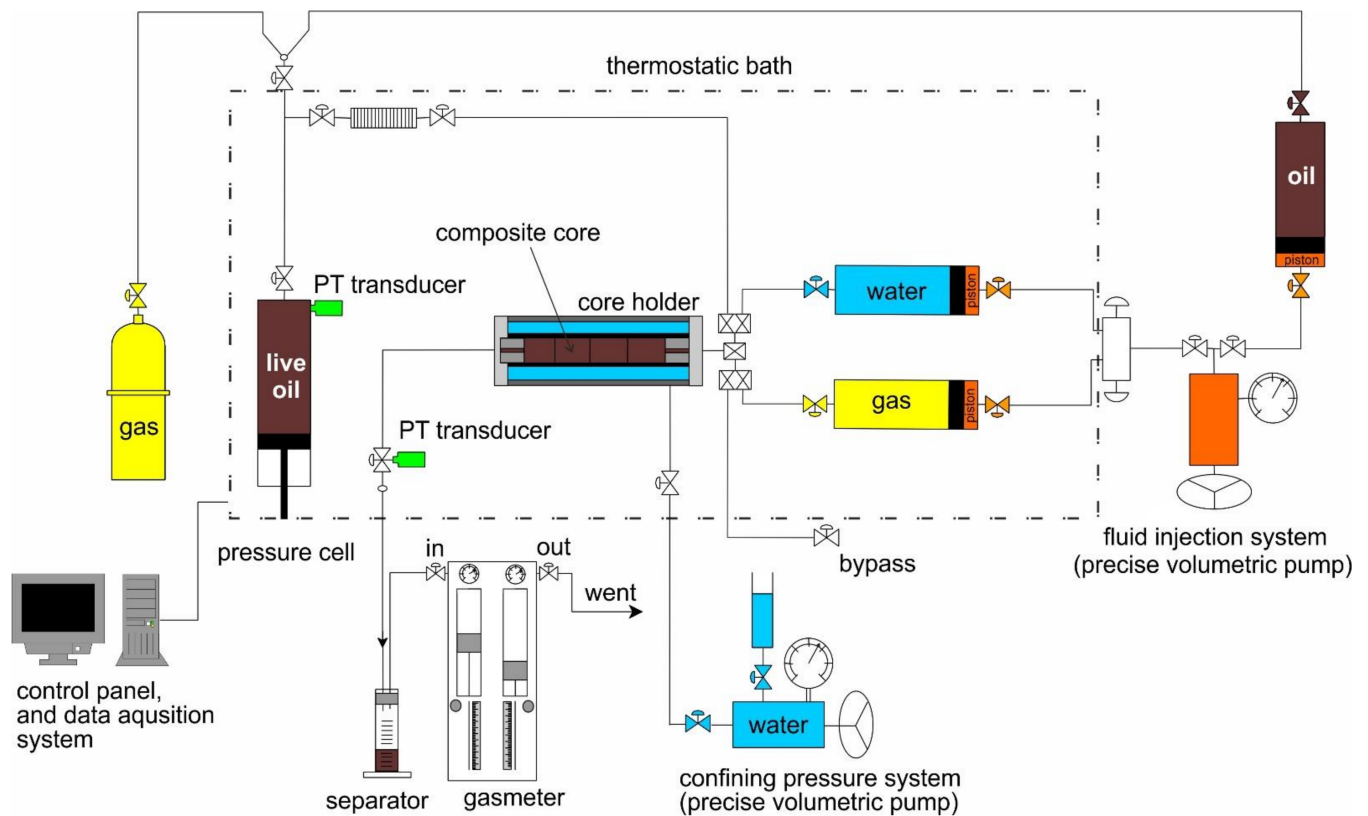


Figure 5. Simplified scheme of the core flooding setup.

Table 9. Core flooding experiments properties.

Test No	Composite Core No	Injection Type	Injected Fluid	WAG Ratio	Number of WAG Cycles	P_i [bar]	S_{wi} [%]	S_{oi} [%]	TWI^1 [PV _{HC}]	TGI^2 [PV _{HC}]
1	6	CGI	CO ₂	0:1	-	270	45.6	54.4	0	1.2
2	2	WAG	CO ₂ /Water	1:1	3	270	53	47	0.6	0.6
3	3	WAG	CO ₂ /Water	2:1	2	270	59.3	40.7	0.8	0.4
4	4	WAG	CO ₂ /Water	1:2	2	270	54.2	45.8	0.4	0.8
5	5	WAG	CO ₂ /Water	1:1	3	170	54.8	45.2	0.6	0.6
6	6	CGI	MG	0:1	-	270	42.1	57.9	0	1.2
7	5	WAG	MG/Water	1:1	3	270	37.1	62.9	0.6	0.6
8	1	WAG	MG/Water	2:1	2	270	43.5	56.5	0.8	0.4
9	2	WAG	MG/Water	1:2	2	270	42.2	57.8	0.4	0.8
10	2	WAG	MG/Water	1:1	3	170	59.5	40.5	0.6	0.6
11	1	CGI	AG	0:1	-	270	40.6	59.4	0	1.2
12	6	WAG	AG/Water	1:1	3	270	41.7	58.3	0.6	0.6
13	3	WAG	AG/Water	2:1	2	270	42.6	57.4	0.8	0.4
14	5	WAG	AG/Water	1:2	2	270	33.4	66.6	0.4	0.8
15	4	WAG	AG/Water	1:1	3	170	38.3	61.7	0.6	0.6
16	5	WAG	KG	1:2	2	270	34.9	65.1	0.4	0.8
17	6	WAG	KG	1:1	3	170	31.7	68.3	0.6	0.6

¹ TWI—total water injected; ² TGI—total gas injected.

2.5. Empirical Correlation for Recovery Factor

Empirical modelling is a process that allows an experimental input–output data set to be transformed into a functional relationship that can be used to estimate results. Genetic programming (GP) uses an evolutionary computation paradigm to generate computer programs that automatically solve a specific problem. Its application involves a transformation of computer programs into a new generation of programs by applying naturally occurring genetic operations [75–77]. Initially, LISP was chosen as the main language for GP in which the program structure is expressed as a parse tree. However, recently many

other modern languages such as Python, Java, C++, and the languages associated with several scientific programming tools (e.g., MATLAB and Mathematica) have been used to develop tree-based GP applications. The variables and constants in the program are leaves of the tree called terminal nodes (terminals), where the arithmetic operations are internal nodes called functions [78]. GP programs can be composed of multiple components (set of trees) grouped under a root node.

Since genetic programming cannot be applied directly to identify nonlinear input–output models, the way to address this problem is to extend GP operators with a tool that uses the Orthogonal Least Squares (OLS) algorithm to create an equation with linear structure described in detail in [79]. Generally, the GP algorithm generates many potential solutions in the form of binary tree structures. These contain terms (subtrees) that affect the accuracy of the model to a greater or lesser extent. The OLS implementation in the GP algorithm involves decomposing tree structures (individual members of population) into subtrees—function terms of the linear in-parameter models. In the next step, the calculation of error reduction ratios of these functions is followed by eliminating the less significant terms. This method, called “tree pruning”, is utilized before the calculation of the fitness values of the trees and conducted in every fitness evaluation. The approach is used to simplify the trees by keeping their accuracy close to the original ones. It is essential to preserve the tree structure because GP works with it. The proposed approach is implemented in the freeware GP-OLS Toolbox available for MATLAB software. This method results in more robust and interpretable models than the classical GP method. To develop a mathematical model, the RF results from core flooding experiments were used. There were seven variables selected, characterizing a given injection scenario, i.e., concentration of components such as CO₂, H₂S, N₂, C₃₊, C₁ in the injected gas, the total share of gas compared to water in the injected fluid stream (Cg), and injection pressure (P). General GP parameters settings are presented in Table 10.

Table 10. GP parameters used in development of the RF correlation.

Parameter	Setting
Population size	1500
Max. tree depth	5
Number of generations (iterations)	500
Generation gap	0.8
Probability of mutation	0.3
Probability of crossover	0.7
Type of selection	Tournament
Type of crossover	One-point
Type of mutation	Randomly selected node
Type of replacement	Least fitness score
Input variables	7

3. Results

3.1. MMP Determination

The slim tube recovery factor for CO₂ obtained from the tests conducted in subsequent pressure steps (Table 8) was in the range of 59.1–97.1%. An example of the slim tube test set in given pressure steps is shown in Figure 6. The results of RF were plotted against pressure, and the MMP was determined using the plot (Figure 7). The pressure determined from the curve break point was 195 bar, while the value corresponding to the RF of 90% was 188 bar. The average, i.e., 192 bar was taken as MMP. The MMP obtained in the PVTsim simulator using the reservoir fluid model was 194 bar.

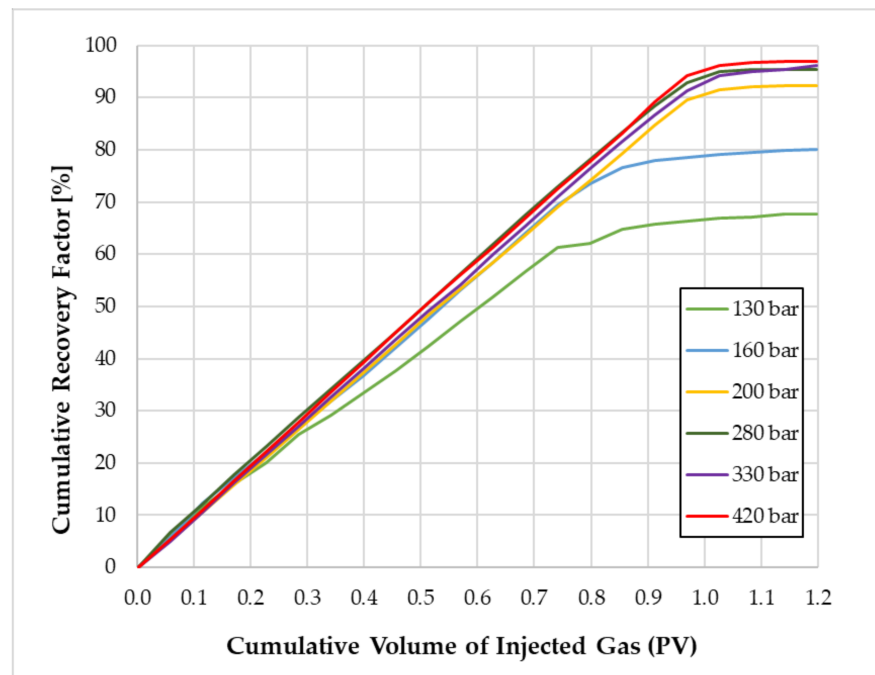


Figure 6. Overview of slim tube recovery factor curves for live oil and CO₂ injected.

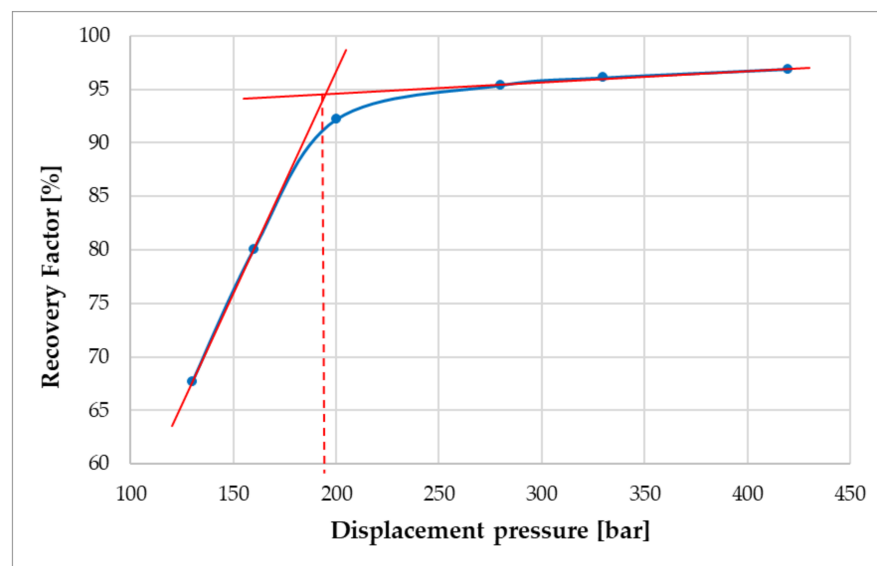


Figure 7. Slim tube recovery factors for CO₂ plotted against pressure—MMP determination.

Similarly, the MMP for acid gas was also determined using the slim tube RF (Figure 8) vs. the displacement pressure plot (Figure 9), and it turned out to be lower than for pure CO₂. The pressure determined from the curve break point was 171 bar, while the value corresponding to the RF of 90% was 173 bar, so the average of 172 bar was taken as MMP. The MMP obtained from simulation, as for pure CO₂ showed very good compliance with the experimental results (174 bar).

Determination of MMP for MG in the considered pressure range based on the slim tube results was impossible. The recovery factor plotted versus pressure follows an almost linear pattern reaching a maximum value of 63% at the highest pressure of 460 bar (Figure 10). For the KG measurement it was omitted because of the much higher nitrogen content of the gas which suggests an even higher MMP value (beyond the testing range). The MMP for KG and MG determined using PVTsim with values of 836 and 1245 bar, respectively, are

surprisingly high and undermine the reliability of the simulations when considering the published data for pure nitrogen, where MMP is generally in the 350–650 bar range [80–83]. Based on the above considerations, it should be concluded that the injection of CO₂ and AG during core flooding will occur in miscible (or near miscible conditions—in the case of experiments conducted at pressure of 170 bar), while high nitrogen gases (MG and KG) are immiscible with reservoir oil in the considered pressure range.

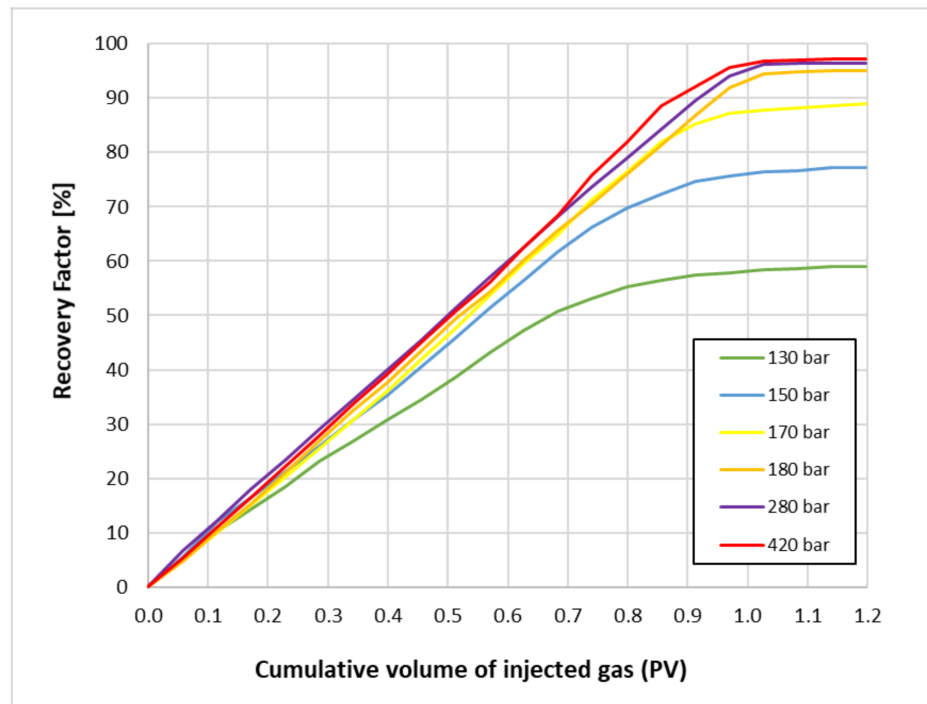


Figure 8. Overview of slim tube recovery factor curves for live oil and AG injected.

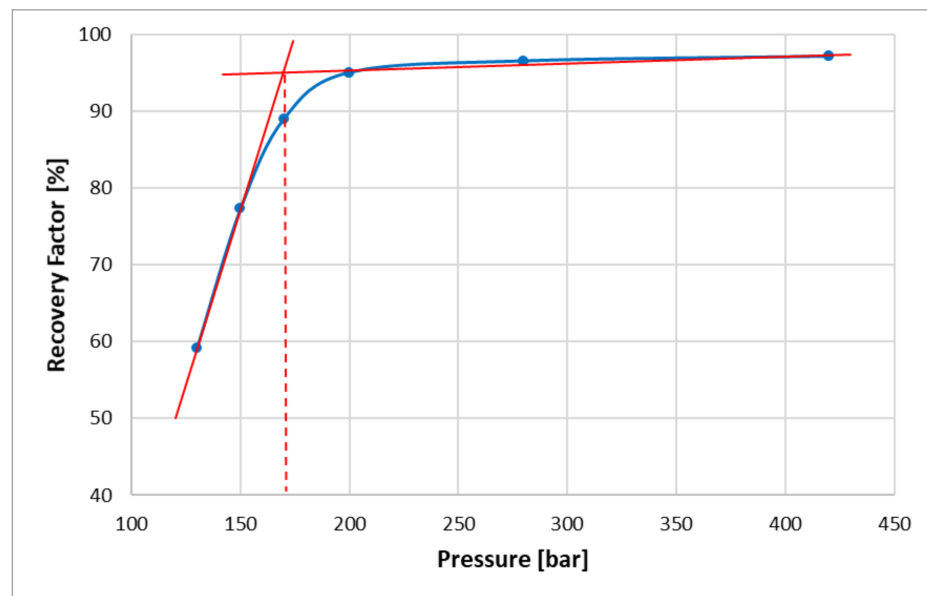


Figure 9. Slim tube recovery factors for H₂S plotted against pressure—MMP determination.

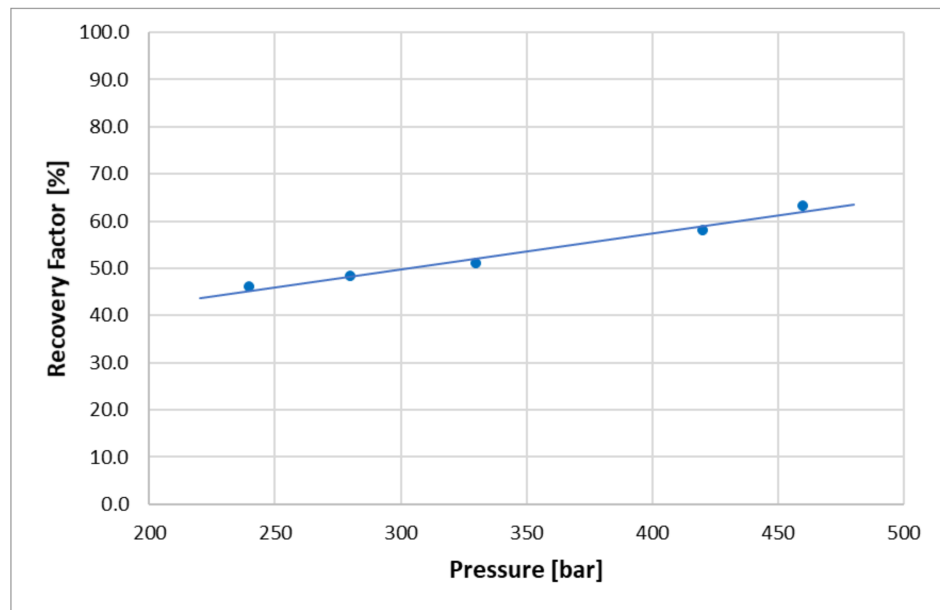


Figure 10. Slim tube recovery factors for MG plotted against pressure.

3.2. Coreflooding

The best efficiency of the WAG process among all the experiments performed was recorded for CO₂, where the recovery factor was in the range of 65.1–82.9% (Figure 11). The application of the WAG process increased the recovery factor by 11.1–28.5 pp when compared to the continuous water injection (CWI). CGI with RF of 79.8% outperformed CWI, and even two WAG schemes (WAG 2:1 at 270 bar, and WAG 1:1 at 170 bar). The highest RF was observed in the WAG 1:2 scheme, where the volume of gas injected within the WAG cycle was two times greater than the water volume. The lowest RF was recorded for the WAG 1:1 scheme conducted at lower pressure (170 bar) accounting for the immiscible nature of the injection process.

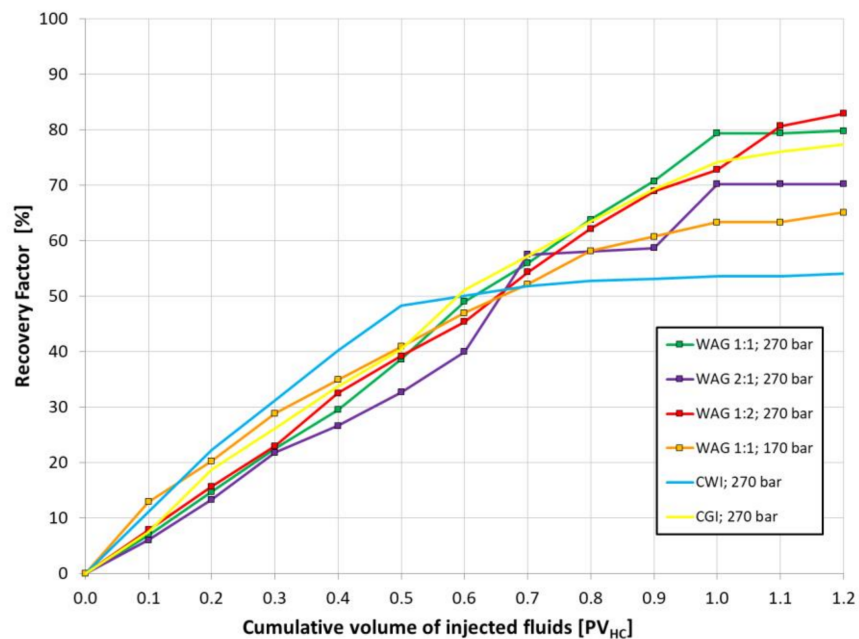


Figure 11. Oil recovery efficiency using different CO₂-WAG schemes compared to CWI and CGI injection.

MG WAG efficiency was considerably lower than that of CO₂-WAG with the RF in the range of 57.1–69.3% (Figure 12). The weakest WAG efficiency was observed in WAG 2:1; 270 bar, with an increased amount of water in the WAG cycle and WAG 1:1; 170 bar, with decreased test pressure. The RF for those injection schemes is only slightly higher than of CWI. The remaining WAG schemes appeared significantly more efficient and resulted in increased RF up to 15 pp. Continuous MG injection turned out to be the least effective injection scheme with RF 10 pp lower than with CWI.

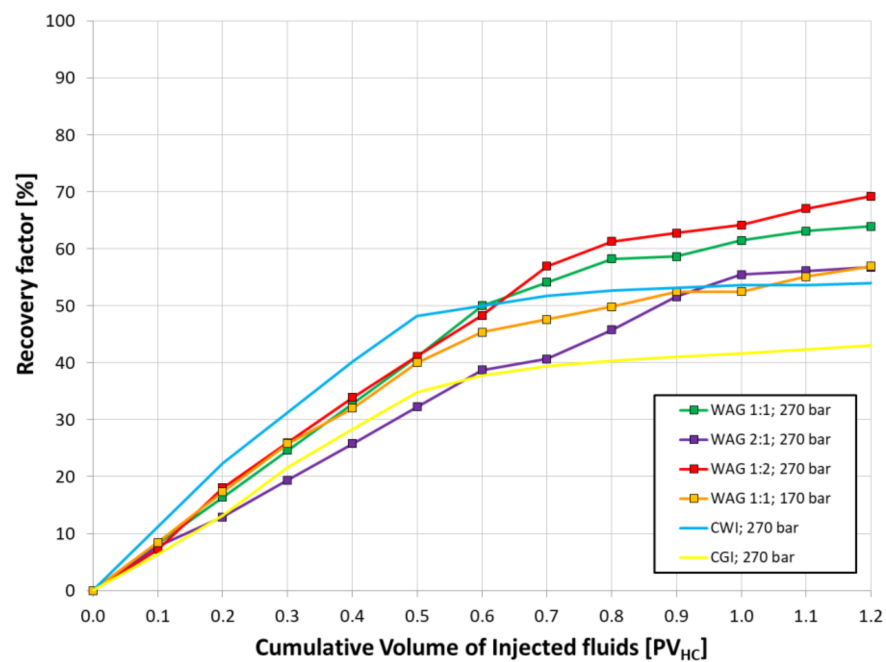


Figure 12. Oil recovery efficiency using MG with different WAG schemes compared to CWI and CGI injection.

Utilization of acid gas in the WAG injection resulted in high recovery factors that are mostly slightly lower than derived by pure CO₂, and definitely higher than derived by KG and MG. The RF of the WAG process was in the range of 60.7–72.6%, indicating an increase vs. CWI of up to 18.6 pp. The highest AG WAG efficiency was observed similar to CO₂ and MG in the WAG 1:2; 270 bar scheme. The lowest WAG efficiency was recorded at reduced test pressure (170 bar). The highest recovery efficiency among the tested schemes was obtained using continuous AG injection with RF of 81.2%. A comparison of different AG injection schemes in relation to CWI expressed in total RF is presented in Figure 13.

The efficiency of KG in the considered WAG injection schemes was in the range of 58.1–72% RF and was much more effective than CGI (RF higher even by 35 pp.) and CWI (RF higher up to 18). The best WAG efficiency was observed for the WAG ratio 1:1, where equal volumes of water and gas were injected in each cycle. The efficiency of WAG with an increased volume of gas compared to water (1:2), and injected at lower pressure was reduced, but still higher than CWI and CGI.

A comparison of different KG injection schemes in relation to CWI expressed in total RF is presented in Figure 14.

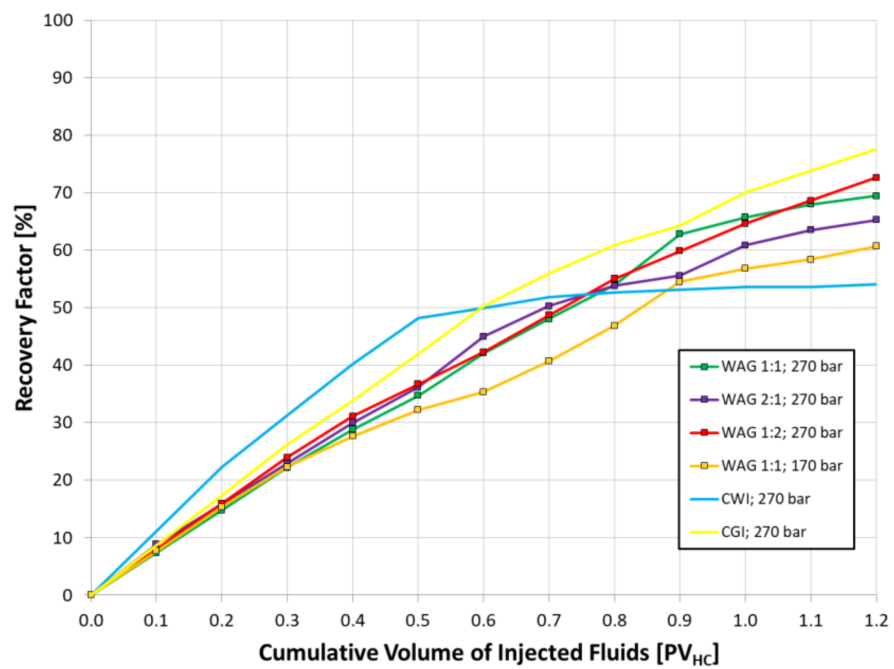


Figure 13. Oil recovery efficiency using AG with different WAG schemes compared to CWI and CGI injection.

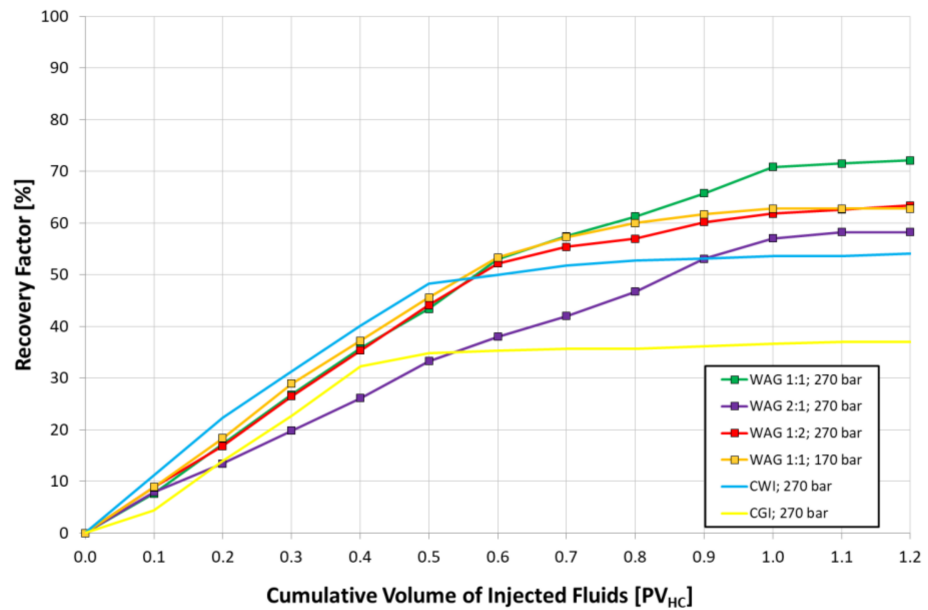


Figure 14. Oil recovery efficiency using KG with different WAG schemes compared to CWI and CGI injection.

3.3. Empirical Modelling

Empirical modelling of RF using GP was based on the experimentally derived RF and other variables characterizing the conducted experiments as gas composition, WAG ratio (reflected as injected gas contribution in the total injected fluids volume), and injection pressure (Table 11).

Table 11. Input and output data used in GP.

Exp No.	Gas	RF from Coreflooding [%]	Variables						
			CO ₂	H ₂ S	N ₂	C ₃₊	C ₁	C _g [%]	P [bar]
1	-	54	0	0	0	0	0	0	270
2	CO ₂	79.8	100	0	0	0	0	50.0	270
3		70.2	100	0	0	0	0	33.3	270
4		82.9	100	0	0	0	0	66.7	270
5		65.1	100	0	0	0	0	50.0	170
6		82.5	100	0	0	0	0	100.0	270
7		GM	43	0.28	3.26	58.5	4.57	28.66	100.0
8	64		0.28	3.26	58.5	4.57	28.66	50.0	270
9	56.8		0.28	3.26	58.5	4.57	28.66	33.3	270
10	69.3		0.28	3.26	58.5	4.57	28.66	66.7	270
11	56.9		0.28	3.26	58.5	4.57	28.66	50.0	170
12	Acid gas (CO ₂ +H ₂ S)	81.2	70	30	0	0	0	100.0	270
13		69.5	70	30	0	0	0	50.0	270
14		65.3	70	30	0	0	0	33.3	270
15		72.6	70	30	0	0	0	66.7	270
16		60.7	70	30	0	0	0	50.0	170
17	GK	37	1.2	2.73	86.85	1.73	5.63	100.0	270
18		72.1	1.2	2.73	86.85	1.73	5.63	50.0	270
19		58.1	1.2	2.73	86.85	1.73	5.63	33.3	270
20		63.4	1.2	2.73	86.85	1.73	5.63	66.7	270
21		62.8	1.2	2.73	86.85	1.73	5.63	50.0	170

Despite the initiation of the algorithm with seven variables, the best fit to the experimental values (95%) was obtained using only five of them. The equation relating the relationship of the RF and the variables characterizing a particular injection scheme takes the following formula:

$$RF = -0.000223 \cdot [(C_{3+} + C_g) \cdot (C_g \cdot N_2)] + 0.088866 \cdot P + 0.189312 \cdot C_g + 0.02397 \cdot (C_g \cdot N_2) - 0.534878 \cdot N_2 + 0.130390 \cdot CO_2 + 28.526032 \quad (1)$$

where:

C₃₊—C₃₊ hydrocarbon fraction content in the injected gas [%]

C_g—Injected gas contribution in the total injected fluid volume [%]

N₂—N₂ content in the injected gas [%]

P—Test pressure [bar]

CO₂—CO₂ content in the injected gas [%]

The fitting of the results derived with a mathematical model presented above to the RF experimental values is presented in Figure 15.

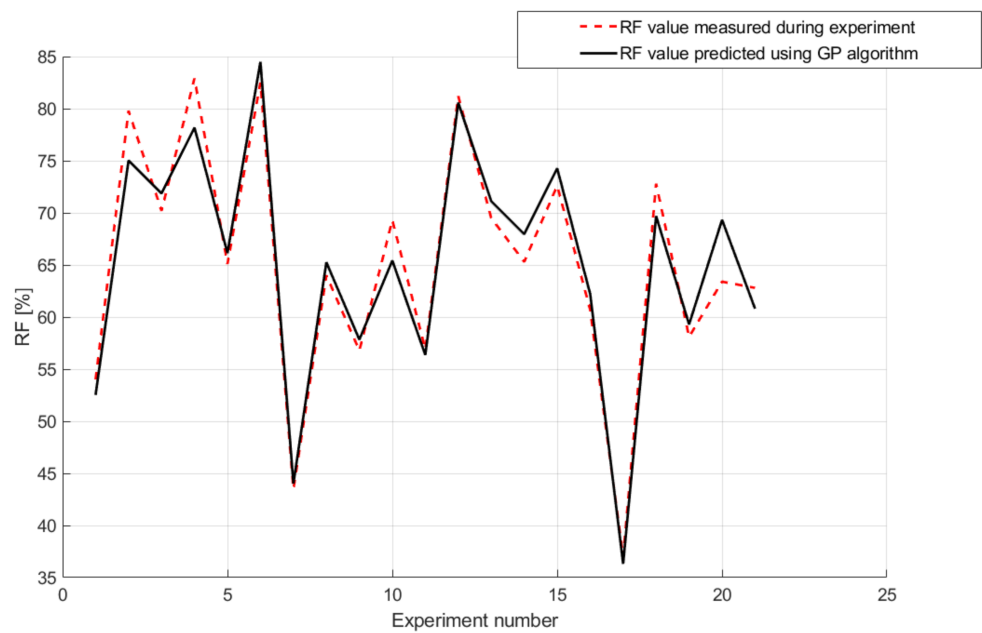


Figure 15. RF model fitting to the experimental results.

The minimum value of the absolute error expressed as the modulus of the difference between calculated and experimentally derived RF is about 0.5 p.p., the maximum value is about 6 p.p. when the average is about 2 p.p. (Figure 16).

A relative error, expressed as the modulus of the absolute error divided by the magnitude of the experimentally derived RF, was also used for the fitting evaluation. The mean relative error was about 3% (Figure 17).

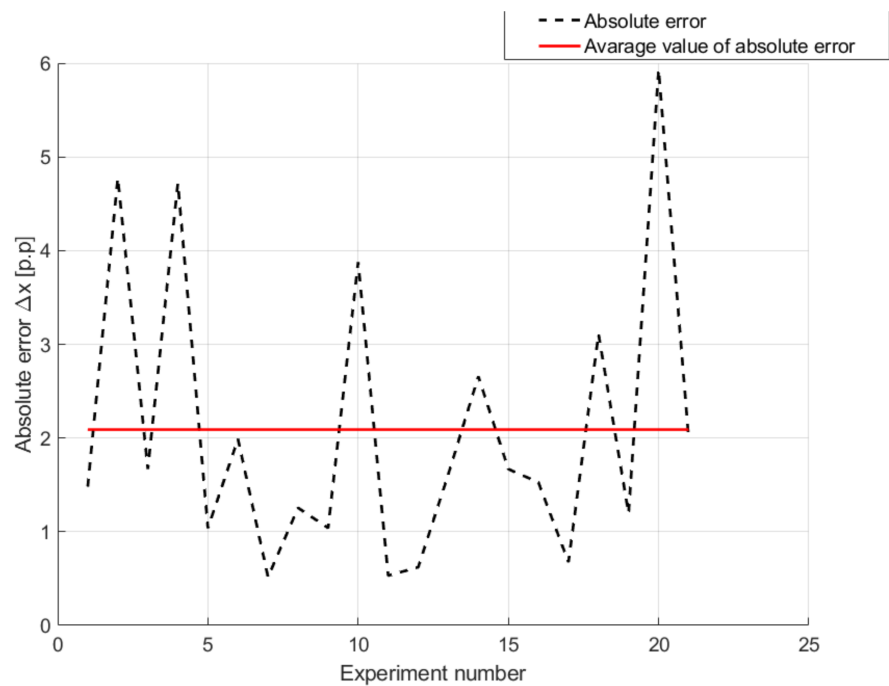


Figure 16. Absolute error.

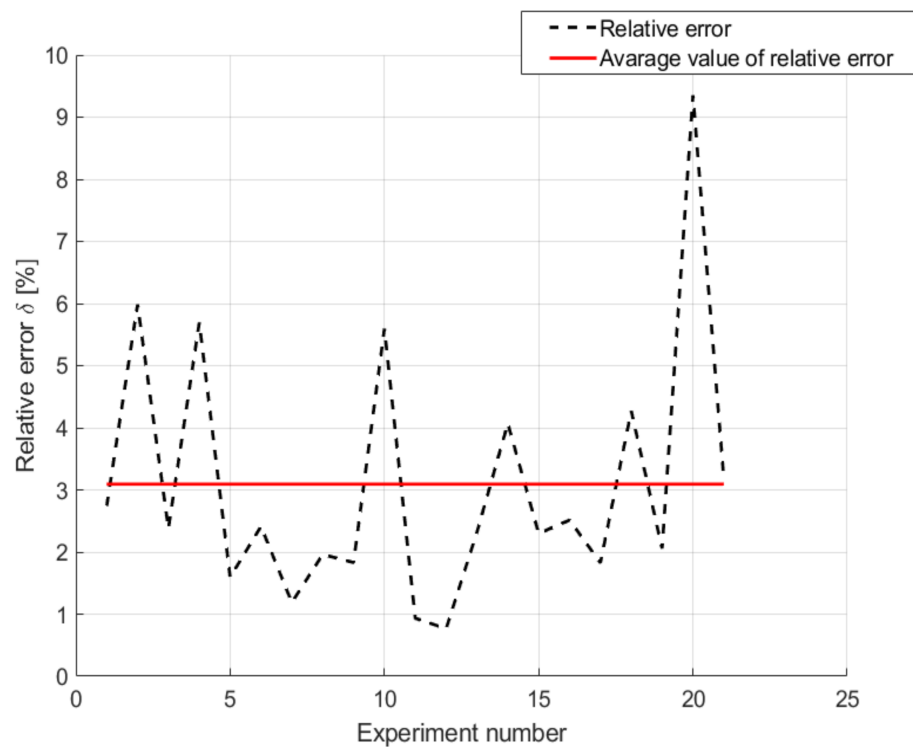


Figure 17. Relative error.

4. Conclusions

An extensive experimental investigation enabled the identification of the efficiency of the WAG method in conditions related to one of most important carbonate oil reservoirs in Poland, and moreover in the determination of the influence of factors such as gas type (composition), WAG ratio, injection pressure, and miscibility of the oil recovery.

The slim tube tests and PVTsim simulations showed that injection of CO₂ and AG during core flooding experiments conducted at 270 bar occurred in miscible conditions. At a lower test pressure of 170 bar, injection of these gases occurred more likely in near-miscible conditions. Injection of the two other gases (MG and KG) occurred in immiscible conditions.

Core flooding studies showed increased efficiency of the WAG process compared to CWI and CGI (except acid gas injection), which were taken as a baseline for evaluating WAG efficiency. As expected, oil recovery efficiency was strongly dependent on the injected gas type and injection parameters (i.e., test pressure, WAG ratio).

The highest WAG efficiencies were observed in scenarios where injection occurred under miscible conditions, i.e., CO₂ and AG. In the most effective injection scheme (CO₂ WAG 1:2, 270 bar), the recovery factor was over 82%, which, compared to CWI, allows the RF to be increased by nearly 30 pp.

The WAG efficiency using high nitrogen natural gases (MG and KG) injected at immiscible conditions was considerably lower, where the most effective schemes resulted in RF of about 70%. The oil recovery was noticeably lower than that obtained with miscible displacement but still significantly higher compared to CWI.

Based on the core flooding results, a mathematical model was constructed for estimating the RF using parameters such as: composition of injected gas, gas contribution in the injected fluid stream, and injection pressure. The equation developed using genetic programming features had a good fit with the experimental result (95%) and can be applied to estimate the RF in conditions specific to domestic oil reservoirs located in the Main Dolomite.

Author Contributions: Conceptualization, M.W. (Miroslaw Wojnicki); methodology, M.W. (Miroslaw Wojnicki) and J.L.; software, M.W. (Miroslaw Wojnicki) and M.G.; validation, J.K.; investigation, M.W. (Miroslaw Wojnicki), M.G., J.K., S.S. and M.W. (Marcin Warnecki); resources, S.S.; writing—original draft preparation, M.W. (Miroslaw Wojnicki); writing—review and editing, M.W. (Miroslaw Wojnicki) and J.L.; supervision, J.L.; project administration, M.W. (Miroslaw Wojnicki). All authors have read and agreed to the published version of the manuscript.

Funding: The work was financially supported by the Polish Ministry of Science and Higher Education (Oil and Gas Institute—National Research Institute Internal Order No. 0033/KB/19 and 0064/KB/20).

Institutional Review Board Statement: Not applicable.

Informed Consent Statement: Not applicable.

Data Availability Statement: Not applicable.

Conflicts of Interest: The authors declare no conflict of interest.

Nomenclature

AG	Acid gas
C_g	Total share of gas in injected fluid stream
CGI	Continuous Gas Injection
CWI	Continuous Water Injection
DI	Deionized water
EOR	Enhanced Oil Recovery
GP	Genetic Programming
IWAG	Immiscible WAG
KG	Very high-nitrogen natural gas
MG	High-nitrogen natural gas
MG	Nitrogen natural gas
MMP	Minimum Miscibility Pressure
nMWAG	Near miscible WAG
OLS	Orthogonal Least Squares
P_i	Injection pressure
pp	Percentage point
PV	Pore Volume
PV_{HC}	Hydrocarbon Pore Volume
RF	Recovery factor
TWI	Total water injected
TGI	Total gas injected
WAG	Water Alternating Gas

References

- McGlade, C.; Sondak, G.; Han, M. Whatever Happened to Enhanced Oil Recovery? International Energy Agency. 2018. Available online: <https://www.iea.org/commentaries/whatever-happened-to-enhanced-oil-recovery> (accessed on 10 January 2022).
- Sheng, J.J. *Enhanced Oil Recovery Field Case Studies*, 1st ed.; Gulf Professional Publishing: Oxford, UK, 2013. [CrossRef]
- Manrique, E.J.; Muci, V.E.; Gurfinkel, M.E. EOR Field Experiences in Carbonate Reservoirs in the United States. *SPE Reserv. Eval. Eng.* **2007**, *10*, 667–686. [CrossRef]
- Alnuaim, S. The Role of R&D in Energy Sustainability: Global Oil and Gas Supply Security and Future Energy Mix. *J. Pet. Technol.* **2019**, *71*, 10–11.
- Kargarpour, M.A. Carbonate reservoir characterization: An integrated approach. *J. Pet. Explor. Prod. Technol.* **2020**, *10*, 2655–2667. [CrossRef]
- Akbar, M.; Vissapragada, B.; Alghamdi, A.H.; Allen, D.; Herron, M.; Carnegie, A.; Dutta, D.; Olesen, J.R.; Chourasiya, R.D.; Logan, D.; et al. A Snapshot of Carbonate Reservoir Evaluation. *Oilfield Rev.* **2000**, *12*, 20–41.
- Jia, C. Petroleum Geology of Carbonate Reservoir. *Adv. Top. Sci. Technol. China* **2012**, 495–532. [CrossRef]
- Huang, Z.; Xing, H.; Zhou, X.; You, H. Numerical study of vug effects on acid-rock reactive flow in carbonate reservoirs. *Adv. Geo-Energy Res.* **2020**, *4*, 448–459. [CrossRef]
- Masalmeh, S.K.; Wei, L.; Blom, C.; Jing, X. EOR Options for Heterogeneous Carbonate Reservoirs Currently under Waterflooding. In Proceedings of the Abu Dhabi International Petroleum Exhibition and Conference, Abu Dhabi, UAE, 10–13 November 2014; Society of Petroleum Engineers: Calgary, AB, Canada, 2014. [CrossRef]

10. Mogensen, K.; Masalmeh, S. A review of EOR techniques for carbonate reservoirs in challenging geological settings. *J. Pet. Sci. Eng.* **2020**, *195*, 107889. [[CrossRef](#)]
11. Jafari, M. Laboratory Study for Water, Gas and WAG Injection in Lab Scale and Core Condition. *Pet. Coal* **2014**, *56*, 175–181.
12. Martyushev, D.A.; Yurikov, A. Evaluation of opening of fractures in the Logovskoye carbonate reservoir, Perm Krai, Russia. *Pet. Res.* **2021**, *6*, 137–143. [[CrossRef](#)]
13. Chichinina, T.I.; Martyushev, D.A. Specific anisotropy properties of fractured reservoirs: Research on Thomsen’s anisotropy parameter delta. In Proceedings of the Geomodel 2021—23th Conference on Oil and Gas Geological Exploration and Development, Gelendzhik, Russia, 6–10 September 2021; Volume 2021, pp. 1–5. [[CrossRef](#)]
14. Manrique, E.J.; Thomas, C.P.; Ravikiran, R.; Izadi, M.; Lantz, M.; Romero, J.L.; Alvaradov, V. EOR: Current status and opportunities. In Proceedings of the SPE Symposium on Improved Oil Recovery, Tulsa, OK, USA, 24–28 April 2010; Society of Petroleum Engineers (SPE): Calgary, AB, Canada, 2010; Volume 2. [[CrossRef](#)]
15. Kulkarni, M.M.; Rao, D.N. Experimental investigation of miscible and immiscible Water-Alternating-Gas (WAG) process performance. *J. Pet. Sci. Eng.* **2005**, *48*, 1–20. [[CrossRef](#)]
16. Christensen, J.R.; Stenby, E.H.; Skauge, A. Review of WAG Field Experience. *SPE Reserv. Eval. Eng.* **2001**, *4*, 97–106. [[CrossRef](#)]
17. Afzali, S.; Rezaei, N.; Zendejboudi, S. A comprehensive review on Enhanced Oil Recovery by Water Alternating Gas (WAG) injection. *Fuel* **2018**, *227*, 218–246. [[CrossRef](#)]
18. Christensen, J.R.; Stenby, E.H.; Skauge, A. Review of WAG Field Experience. In Proceedings of the International Petroleum Conference and Exhibition of Mexico, Villahermosa, Mexico, 3–5 March 1998; Society of Petroleum Engineers: Calgary, AB, Canada, 1998. [[CrossRef](#)]
19. Teigland, R.; Kleppe, J. EOR Survey in the North Sea. In Proceedings of the SPE/DOE Symposium on Improved Oil Recovery, Tulsa, OK, USA, 22–26 April 2006; Society of Petroleum Engineers: Calgary, AB, Canada, 2006. [[CrossRef](#)]
20. Surguchev, L.M.; Korbel, R.; Haugen, S.; Krakstad, O.S. Screening of WAG Injection Strategies for Heterogeneous Reservoirs. In Proceedings of the European Petroleum Conference, Cannes, France, 16–18 November 1992. [[CrossRef](#)]
21. Skauge, A.; Serbie, K. Status of fluid flow mechanisms for miscible and immiscible WAG. In Proceedings of the Society of Petroleum Engineers—SPE EOR Conference at Oil and Gas West Asia 2014: Driving Integrated and Innovative EOR, Muscat, Oman, 31 March–2 April 2014; Society of Petroleum Engineers: Calgary, AB, Canada, 2014. [[CrossRef](#)]
22. Caudle, B.H.; Dyes, A.B. Improving Miscible Displacement by Gas-Water Injection. *Trans. AIME* **1958**, *213*, 281–283. [[CrossRef](#)]
23. Lin, E.C.; Poole, E.S. Numerical evaluation of single-slug, WAG, and hybrid CO₂ injection processes, Dollarhide Devonian Unit, Andrews County, Texas. *SPE Reserv. Eng.* **1991**, *6*, 415–420. [[CrossRef](#)]
24. Khan, M.Y.; Kohata, A.; Patel, H.; Syed, F.I.; Al Sowaidi, A.K. Water alternating gas WAG optimization using tapered WAG technique for a giant offshore middle east oil field. In Proceedings of the Society of Petroleum Engineers—Abu Dhabi International Petroleum Exhibition and Conference 2016, Abu Dhabi, UAE, 7 November 2016; Society of Petroleum Engineers: Calgary, AB, Canada, 2016; Volume 2016. [[CrossRef](#)]
25. Fatemi, S.M.; Sohrabi, M. Experimental Investigation of Near-Miscible Water-Alternating-Gas Injection Performance in Water-Wet and Mixed-Wet Systems. *SPE J.* **2013**, *18*, 114–123. [[CrossRef](#)]
26. Lubaś, J.; Stopa, J.; Wojnicki, M. Możliwości zastosowania zaawansowanych metod wspomaganie wydobywania ropy naftowej ze złóż dojrzałych. *Naft.-Gaz* **2019**, *75*, 24–28. [[CrossRef](#)]
27. Ma, T.D.; Youngren, G.K. Performance of Immiscible Water-Alternating-Gas (IWAG) Injection at Kuparuk River Unit, North Slope, Alaska. In Proceedings of the SPE Annual Technical Conference and Exhibition, New Orleans, LA, USA, 25 September 1994; Society of Petroleum Engineers: Calgary, AB, Canada, 1994. [[CrossRef](#)]
28. Ramachandran, K.P.; Gyani, O.N.; Sur, S. Immiscible Hydrocarbon WAG: Laboratory to Field. In Proceedings of the SPE Oil and Gas India Conference and Exhibition, Mumbai, India, 20–22 January 2010; Society of Petroleum Engineers (SPE): Calgary, AB, Canada, 2010. [[CrossRef](#)]
29. Agbalaka, C.C.; Dandekar, A.Y.; Patil, S.L.; Khataniar, S.; Hemsath, J. The Effect Of Wettability On Oil Recovery: A Review. In Proceedings of the SPE Asia Pacific Oil and Gas Conference and Exhibition, Perth, Australia, 20–22 October 2008; Society of Petroleum Engineers: Calgary, AB, Canada, 2008. [[CrossRef](#)]
30. Huang, E.T.S.; Holm, L.W. Effect of WAG injection and rock wettability on oil recovery during CO₂ flooding. *SPE Reserv. Eng.* **1988**, *3*, 119–129. [[CrossRef](#)]
31. Hoare, G.; Coll, C. Effect of small/medium scale reservoir heterogeneity on the effectiveness of water, gas and water alternating gas WAG injection. In Proceedings of the Society of Petroleum Engineers—SPE Europec featured at 80th EAGE Conference and Exhibition 2018, Copenhagen, Denmark, 11–14 June 2018; Society of Petroleum Engineers: Calgary, AB, Canada, 2018. [[CrossRef](#)]
32. Speight, J.G. *Introduction to Enhanced Recovery Methods for Heavy Oil and Tar Sands*; Elsevier: Amsterdam, The Netherlands, 2016. [[CrossRef](#)]
33. van Lingen, P.P.; Barzanji, O.H.M.; van Kruijsdijk, C.P.J.W. WAG Injection to Reduce Capillary Entrapment in Small-Scale Heterogeneities. In Proceedings of the SPE Annual Technical Conference and Exhibition, Denver, CO, USA, 6 October 1996; Society of Petroleum Engineers: Calgary, AB, Canada, 1996. [[CrossRef](#)]
34. Kharrat, R.; Mahdavi, S.; Ghorbani, D. A Comprehensive EOR Study of a Highly Fractured Matured Field-Case Study. In Proceedings of the SPE Europec/EAGE Annual Conference, Copenhagen, Denmark, 4–7 June 2012; Society of Petroleum Engineers: Calgary, AB, Canada, 2012. [[CrossRef](#)]

35. Dang, C.; Nghiem, L.; Nguyen, N.; Chen, Z.; Nguyen, Q. Evaluation of CO₂ Low Salinity Water-Alternating-Gas for enhanced oil recovery. *J. Nat. Gas Sci. Eng.* **2016**, *35*, 237–258. [[CrossRef](#)]
36. Motealleh, M.; Kharrat, R.; Hashemi, A. An experimental investigation of water-alternating-CO₂ coreflooding in a carbonate oil reservoir in different initial core conditions. *Energy Sources Part A Recovery Util. Environ. Eff.* **2013**, *35*, 1187–1196. [[CrossRef](#)]
37. Teklu, T.W.; Alameri, W.; Graves, R.M.; Kazemi, H.; AlSumaiti, A.M. Low-salinity water-alternating-CO₂ EOR. *J. Pet. Sci. Eng.* **2016**, *142*, 101–118. [[CrossRef](#)]
38. Ghafoori, A.; Shahbazi, K.; Darabi, A.; Soleymanzadeh, A.; Abedini, A. The experimental investigation of nitrogen and carbon dioxide water-alternating-gas injection in a carbonate reservoir. *Pet. Sci. Technol.* **2012**, *30*, 1071–1081. [[CrossRef](#)]
39. Al-Shuraiqi, H.S.; Muggeridge, A.H.; Grattoni, C.A. Laboratory Investigations of First Contact Miscible WAG Displacement: The Effects of WAG Ratio And Flow Rate. In Proceedings of the SPE International Improved Oil Recovery Conference in Asia Pacific, Kuala Lumpur, Malaysia, 20 October 2003; Society of Petroleum Engineers: Calgary, AB, Canada, 2003. [[CrossRef](#)]
40. Juanes, R.; Blunt, M.J. Impact of viscous fingering on the prediction of optimum WAG ratio. *SPE J.* **2007**, *12*, 486–495. [[CrossRef](#)]
41. Rahimi, V.; Bidarigh, M.; Bahrami, P. Experimental Study and Performance Investigation of Miscible Water-Alternating-CO₂ Flooding for Enhancing Oil Recovery in the Sarvak Formation. *Oil Gas Sci. Technol.—Rev. d’IFP Energies Nouv.* **2017**, *72*, 35. [[CrossRef](#)]
42. Wojnicki, M. Experimental investigations of oil displacement using the WAG method with carbon dioxide. *Naft.-Gaz* **2017**, *73*, 864–870. [[CrossRef](#)]
43. Jiang, H.; Nuryaningsih, L.; Adidharma, H. The study of timing of cyclic injections in miscible CO₂ WAG. In Proceedings of the Society of Petroleum Engineers Western Regional Meeting 2012, Bakersfield, CA, USA, 21 March 2012; Society of Petroleum Engineers: Calgary, AB, Canada, 2012. [[CrossRef](#)]
44. Shahverdi, H.; Sohrabi, M.; Fatemi, M.; Jamiolahmady, M. Three-phase relative permeability and hysteresis effect during WAG process in mixed wet and low IFT systems. *J. Pet. Sci. Eng.* **2011**, *78*, 732–739. [[CrossRef](#)]
45. Fatemi, S.M.; Sohrabi, M. Cyclic hysteresis of three-phase relative permeability curves applicable to WAG injection under low gas/oil IFT: Effect of immobile water saturation, injection scenario and rock permeability. In Proceedings of the 75th European Association of Geoscientists and Engineers Conference and Exhibition 2013 Incorporating SPE EUROPEC 2013: Changing Frontiers, European Association of Geoscientists and Engineers, EAGE, London, UK, 10 June 2013. [[CrossRef](#)]
46. Sohrabi, M.; Danesh, A.; Jamiolahmady, M. Visualisation of residual oil recovery by near-miscible gas and SWAG injection using high-pressure micromodels. *Transp. Porous Media* **2008**, *74*, 239–257. [[CrossRef](#)]
47. Sohrabi, M.; Tehrani, D.H.; Danesh, A.; Henderson, G.D. Visualization of oil recovery by water-alternating-gas injection using high-pressure micromodels. *SPE J.* **2004**, *9*, 290–301. [[CrossRef](#)]
48. Dong, M.; Foraja, J.; Huang, S.; Chatzis, I. Analysis of immiscible Water-Alternating-Gas (WAG) injection using micromodel tests. *J. Can. Pet. Technol.* **2005**, *44*, 17–24. [[CrossRef](#)]
49. Larsen, J.K.; Bech, N.; Winter, A. Three-Phase Immiscible WAG Injection: Micromodel Experiments and Network Models. In Proceedings of the SPE/DOE Improved Oil Recovery Symposium, Tulsa, OK, USA, 3–5 April 2000; Society of Petroleum Engineers (SPE): Calgary, AB, Canada, 2000. [[CrossRef](#)]
50. Wojnicki, M.; Lubás, J.; Warnecki, M.; Kúsniarczyk, J.; Szuflita, S. Experimental studies of immiscible high-nitrogen natural gas WAG injection efficiency in mixed-wet carbonate reservoir. *Energies* **2020**, *13*, 2346. [[CrossRef](#)]
51. Luchian, H.; Băutu, A.; Băutu, E. Genetic programming techniques with applications in the oil and gas industry. In *Artificial Intelligent Approaches in Petroleum Geosciences*; Springer International Publishing: Berlin/Heidelberg, Germany, 2015. [[CrossRef](#)]
52. Velez-Langs, O. Genetic algorithms in oil industry: An overview. *J. Pet. Sci. Eng.* **2005**, *47*, 15–22. [[CrossRef](#)]
53. Jensen, J.P.; Andersen, M.G. *Reservoir Production Optimization Using Genetic Algorithms and Artificial Neural Networks*; Downing, K., Ed.; Institutt for datateknologi og informatikk: Trondheim, Norway, 2009.
54. Soleng, H.H. Oil reservoir production forecasting with uncertainty estimation using genetic algorithms. In Proceedings of the 1999 Congress on Evolutionary Computation, CEC 1999, Washington, DC, USA, 6–9 July 1999; IEEE Computer Society: Washington, DC, USA, 1999; Volume 2. [[CrossRef](#)]
55. Vo Thanh, H.; Sugai, Y.; Nguele, R.; Sasaki, K. Robust optimization of CO₂ sequestration through a water alternating gas process under geological uncertainties in Cuu Long Basin, Vietnam. *J. Nat. Gas Sci. Eng.* **2020**, *76*, 103208. [[CrossRef](#)]
56. Safarzadeh, M.A.; Motahhari, S.M. Co-optimization of carbon dioxide storage and enhanced oil recovery in oil reservoirs using a multi-objective genetic algorithm (NSGA-II). *Pet. Sci.* **2014**, *11*, 460–468. [[CrossRef](#)]
57. Mohagheghian, E.; James, L.A.; Haynes, R.D. Optimization of hydrocarbon water alternating gas in the Norne field: Application of evolutionary algorithms. *Fuel* **2018**, *223*, 86–98. [[CrossRef](#)]
58. Nait Amar, M.; Zeraibi, N.; Redouane, K. Optimization of WAG Process Using Dynamic Proxy, Genetic Algorithm and Ant Colony Optimization. *Arab. J. Sci. Eng.* **2018**, *43*, 6399–6412. [[CrossRef](#)]
59. Janiga, D.; Czarnota, R.; Stopa, J.; Wojnarowski, P. Huff and puff process optimization in micro scale by coupling laboratory experiment and numerical simulation. *Fuel* **2018**, *224*, 289–301. [[CrossRef](#)]
60. Khan, M.R.; Kalam, S.; Khan, R.A.; Tariq, Z.; Abdulraheem, A. Comparative analysis of intelligent algorithms to predict the minimum miscibility pressure for hydrocarbon gas flooding. In Proceedings of the Society of Petroleum Engineers—Abu Dhabi International Petroleum Exhibition and Conference 2019, ADIP 2019, Abu Dhabi, UAE, 11–14 November 2019; Society of Petroleum Engineers: Calgary, AB, Canada, 2019. [[CrossRef](#)]

61. Mahdiani, M.R.; Kooti, G. The most accurate heuristic-based algorithms for estimating the oil formation volume factor. *Petroleum* **2016**, *2*, 40–48. [[CrossRef](#)]
62. Nasery, S.; Hoseinpour, S.; Phung, L.T.K.; Bahadori, A. Prediction of the viscosity of water-in-oil emulsions. *Pet. Sci. Technol.* **2016**, *34*, 1972–1977. [[CrossRef](#)]
63. Tukur, A.D.; Nzerem, P.; Nsan, N.; Okafor, I.S.; Gimba, A.; Ogolo, O.; Oluwaseun, A.; Andrew, O. Well placement optimization using simulated annealing and genetic algorithm. In Proceedings of the Society of Petroleum Engineers—SPE Nigeria Annual International Conference and Exhibition 2019, NAIC 2019, Lagos, Nigeria, 5–7 August 2019; Society of Petroleum Engineers: Calgary, AB, Canada, 2019. [[CrossRef](#)]
64. Li, H.; Yu, H.; Cao, N.; Tian, H.; Cheng, S. Applications of Artificial Intelligence in Oil and Gas Development. *Arch. Comput. Methods Eng.* **2020**, *28*, 937–949. [[CrossRef](#)]
65. López, S.; Koç, U.; Bakker, E.; Rahmani, J. Optimization of Lift Gas Allocation Using Evolutionary Algorithms. *Int. J. Comput. Appl. Technol. Res.* **2019**, *8*, 353–357. [[CrossRef](#)]
66. Andreasen, A. Applied Process Simulation-Driven Oil and Gas Separation Plant Optimization Using Surrogate Modeling and Evolutionary Algorithms. *ChemEngineering* **2020**, *4*, 11. [[CrossRef](#)]
67. De Pádua, L.; Sales, A.; Ramalho Pitombeira-Neto, A.; De Athayde Prata, B. A genetic algorithm integrated with Monte Carlo simulation for the field layout design problem. *Oil Gas Sci. Technol.—Rev. d'IFP Energies Nouv.* **2018**, *73*, 24. [[CrossRef](#)]
68. American Petroleum Institute (API). *Sampling Petroleum Reservoir Fluids*; API Recommended Practice 2003; American Petroleum Institute (API): Washington, DC, USA, 2003; Volume 44.
69. Langaas, K.; Ekrann, S.; Ebeltoft, E. A criterion for ordering individuals in a composite core. *J. Pet. Sci. Eng.* **1998**, *19*, 21–32. [[CrossRef](#)]
70. Piñerez, I.; Puntervold, T.; Strand, S.; Hopkins, P.; Aslanidis, P.; Yang, H.S.; Kinn, M.S. Core wettability reproduction: A new solvent cleaning and core restoration strategy for chalk cores. *J. Pet. Sci. Eng.* **2020**, *195*, 107654. [[CrossRef](#)]
71. Holtz, M.H. Immiscible water alternating gas (IWAG) EOR: Current state of the art. In Proceedings of the SPE—DOE Improved Oil Recovery Symposium, Tulsa, OK, USA, 11 April 2016; Society of Petroleum Engineers (SPE): Calgary, AB, Canada, 2016; Volume 2016. [[CrossRef](#)]
72. Holm, L.W.; Josendal, V.A. Effect of Oil Composition on Miscible-Type Displacement by Carbon Dioxide. *Soc. Pet. Eng. J.* **1982**, *22*, 87–98. [[CrossRef](#)]
73. Holm, L.W. Miscibility and Miscible Displacement. *J. Pet. Technol.* **1986**, *38*, 817–818. [[CrossRef](#)]
74. Whitson, C.H.; Brulé, M.R. Phase behavior. *SPE Monogr. Ser.* **2000**, *20*, 233.
75. Koza, J.R. Genetic programming as a means for programming computers by natural selection. *Stat. Comput.* **1994**, *4*, 87–112. [[CrossRef](#)]
76. Koza, J.R.; Poli, R. Genetic Programming. In *Search Methodologies: Introductory Tutorials in Optimization and Decision Support Techniques*; Springer: Berlin/Heidelberg, Germany, 2005; pp. 127–164. [[CrossRef](#)]
77. Sette, S.; Boullart, L. Genetic programming: Principles and applications. *Eng. Appl. Artif. Intell.* **2001**, *14*, 727–736. [[CrossRef](#)]
78. Poli, R.; Langdon, W.B.; Mcphee, N.F.; Koza, J.R. *A Field Guide to Genetic Programming*. 2008. Available online: <http://www.gp-field-guide.org.uk> (accessed on 15 October 2021).
79. Madár, J.; Abonyi, J.; Szeifert, F. Genetic Programming for the Identification of Nonlinear Input–Output Models. *Ind. Eng. Chem. Res.* **2005**, *44*, 3178–3186. [[CrossRef](#)]
80. Glaso, O. Miscible displacement: Recovery Tests Nitrogen. *SPE Reserv. Eng. Soc. Pet. Eng.* **1990**, *5*, 61–68. [[CrossRef](#)]
81. Sebastian, H.M.; Lawrence, D.D. Nitrogen Minimum Miscibility Pressures. In Proceedings of the SPE/DOE Enhanced Oil Recovery Symposium, Tulsa, OK, USA, 22–24 April 1992; Society of Petroleum Engineers: Calgary, AB, Canada, 1992. [[CrossRef](#)]
82. Anada, H.R. *State-of-the-Art Review of Nitrogen and Flue Gas Flooding in Enhanced Oil Recovery*; Final Report; Science Applications, Inc.: Pittsburgh, PA, USA; Morgantown, WV, USA, 1980. [[CrossRef](#)]
83. Hudgins, D.A.; Llave, F.M.; Chung, F.T.H. Nitrogen Miscible Displacement of Light Crude Oil: A Laboratory Study. *SPE Reserv. Eng.* **1990**, *5*, 100–106. [[CrossRef](#)]